

Co-TPP functionalized carbon nanotube composites for detection of nitrobenzene and chlorobenzene vapours

SWASTI SAXENA¹, G S S SAINI² and A L VERMA^{1,*}

¹Amity Institute of Applied Sciences, Amity University, Noida 201 303 (U.P.), India

²Department of Physics, Punjab University, Chandigarh 160 014, India

MS received 21 July 2014; revised 30 September 2014

Abstract. We report preparation of nanocomposites by non-covalent functionalization of carbon nanotubes (CNTs) with metal-tetraphenylporphyrins (M-TPP). Fourier transform infrared (FTIR) spectroscopy and transmission electron microscopy (TEM) results suggest formation of nanosized clusters of Co-TPP around the CNTs surface. X-ray diffraction studies indicate electronic charge re-distribution and strong interactions among CNTs and Co-TPP on functionalization. The films of the hybrid CNT–M-TPP nanocomposite exhibit change in conductivity on exposure to some chemical vapours. In the present work, the films prepared from the cobalt-TPP functionalized CNTs hybrid composites have been investigated for the detection of chlorobenzene (CB) and nitrobenzene (NB) vapours at room temperature. The films show response time of few seconds on exposure to both the NB and CB vapours while the recovery time for NB is significantly different compared to CB. A distinct and highly reproducible response pattern in the relative changes in resistance, recovery and response times on exposure to the vapours of NB, CB and few other chemicals at room temperature has been exploited to differentiate CB and NB vapours from one another.

Keywords. Electrical properties; nanostructure materials; porphyrin functionalized carbon nanotubes; sensor for chlorobenzene and nitrobenzene vapour.

1. Introduction

The halogenated and nitro-aromatic compounds are widely used in many industrial processes. Nitrobenzene (NB) is an important raw material and solvent used in the manufacture of aniline,¹ dyes, pesticides, explosives, lubricating oils, synthetic rubber, pharmaceuticals, etc.^{2–4}

On the other hand, chlorobenzene (CB) is used extensively as a solvent, heat transfer agent, insect repellent, deodorant and as intermediate in the synthesis of dyes and pesticides.⁵ The extensive use of the nitro-, and halogenated benzenes have led to their widespread release in the environment causing pollution,⁶ are carcinogenic and serious health hazard.⁷

Because of the acute toxicity and health hazard posed from NB and CB, their careful monitoring in industries and environment is very important. UV–visible spectroscopy,⁸ chromatography, mass spectrometry and gas chromatography-based detectors^{9–12} are sensitive and quite accurate, but they are either bulky or expensive, and time consuming in interpreting data. In comparison, chemical sensors are small in size, inexpensive and can be used in portable and real-time monitoring devices.¹³ Out of various kinds of sensors, the development of chemiresistive sensors and devices^{14,15} based on nanomaterials are being explored as

potential sensor materials for different analytes due to their unique electronic, physical and chemical properties.

In order to overcome the serious drawback of poor selectivity of pristine multiwalled nanotube (MWNT), surface modifications of MWNT and grafting with different functional groups to improve sensitivity and selectivity towards specific analytes are being vigorously pursued. In this effort, an array of MWNT decorated with nanoclusters of different noble metals have been used to enhance sensitivity of MWNT for some gases operating at sensor temperatures of 100–200°C.^{15–17}

During recent past, interesting class of compounds called porphyrins and metal–porphyrins have emerged as very attractive functional materials possessing multiple recognition properties. The adsorption and reactivity of analytes with metal–porphyrins can be tuned by either selecting different metals at the centre and/or substituents at the porphyrin periphery which can provide selectivity to the sensors made from such materials. In recent times, the authors¹⁸ have demonstrated fabrication of a very selective and sensitive device made from cobalt-, and copper-phthalocyanine (M-Pc) functionalized MWNT for detection of H₂O₂ in the vapour form. On the other hand, Penza *et al*^{16,17,19} have used surface modified MWNT with different metal–porphyrins and their derivatives as functional materials for detection of few volatile compounds while studies on sensing of tetrafluoroquinone functionalized carbon nanotubes (CNTs)

*Author for correspondence (alverma@amity.edu; alverma@yahoo.com)

for formaldehyde,²⁰ and Fe-TPP functionalized MWNT for benzene²¹ have been reported. Thus M-TPP functionalized MWNT is emerging a very active research area in the field of detection of chemical vapours.

In this paper, we report preparation of nanocomposites by non-covalent functionalization of MWNT with metal-tetraphenylporphyrins by blending and ultrasonification of MWNT with M-TPP in toluene or ethanol. The morphology and structure of the composites were investigated using Fourier transform infrared (FTIR), X-ray diffraction (XRD), scanning and transmission electron microscopy (SEM and TEM) techniques. The FTIR and TEM results suggest the formation of nanosized clusters of aggregated M-TPP around MWNT surface. The conjugative electronic structure of M-TPP is expected to facilitate adsorption of ring compounds like CB, NB, etc. onto the surface of M-TPP through π - π , van der Waals and other non-covalent interactions.

2. Experimental

2.1 Preparation of composites and sensors

Multiwalled carbon nanotubes and M-TPP were purchased from Sigma Chemical Co. Commercially available spectroscopic grade solvents and chemicals were employed in our experiments.

In order to overcome the poor chemical reactivity of pristine MWNTs, they were subjected to corona electrostatic discharge¹⁸ which resulted in the grafting of -OH groups to the end faces and defect sites on the walls of MWNTs. This is confirmed by the presence of bands around 3436 and 1627 cm^{-1} in the FTIR spectra of f-MWNTs resulting from O-H stretching and deformation modes, respectively, as shown in figure 1. These -OH group grafted MWNTs show enhanced chemical reactivity and thus were used for non-covalent functionalization with M-TPP using the blending and ultrasonification procedure reported by us.^{18,22} We prepared samples by using different quantities of Co-TPP and f-MWNTs. The prepared composites showed widely different resistivities depending upon the relative quantities of M-TPP and f-MWNT. We used only those composites which showed resistivity in the $\text{k}\Omega$ cm range for ease in measurements. We adopted a similar procedure for the preparation of stable films of hybrid nanocomposites and measurement of conductivity on exposure to various vapours as discussed in our earlier work.²²

2.2 Measurements

The gas-sensitive characteristics of the composites films were investigated at ambient conditions by recording their electrical responses when exposed alternately to the purified N_2 gas and chemical vapours under investigation. On the basis of partial pressure of gases and flow rate of nitrogen gas, it was possible to vary the concentration of NB or CB from ~ 5 to ~ 250 ppm range. The outlet for chemical

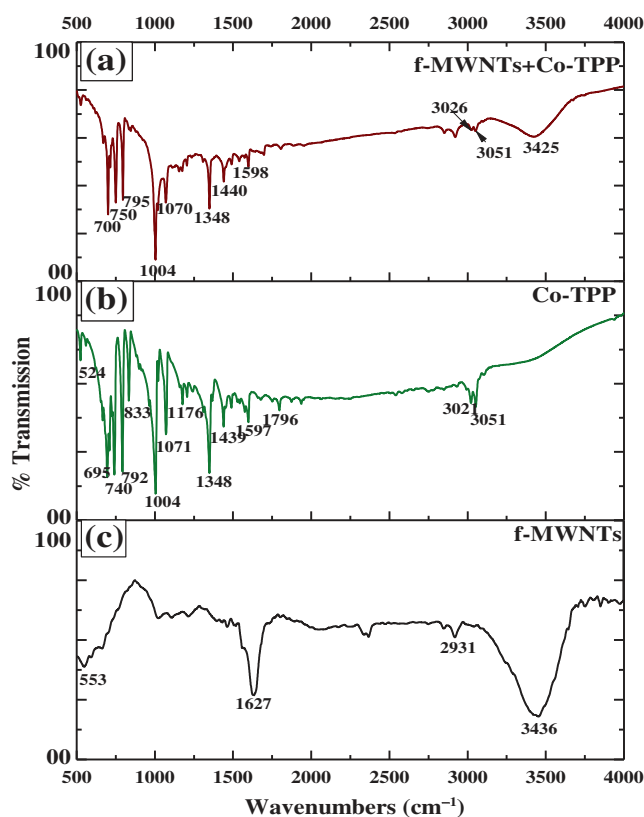


Figure 1. Fourier-transform infrared spectra of f-MWNT; pure Co-TPP and f-MWNT+Co-TPP composite from 500 to 4000 cm^{-1} . For comparison purposes important bands are marked.

vapours was closed after one second, purged with nitrogen gas to allow the resistance of the sensor to recover to original value. The electrical current and resistance of the films were measured by a volt-amperometric technique in a two-pole format using Keithley Model 6517B electrometer interfaced with a computer to store and process the data.

2.3 Experimental procedure

The samples of pristine f-MWNT, pure M-TPP and nanocomposites prepared by functionalization of MWNT with M-TPP were diluted in KBr matrix to measure FTIR spectra on a Perkin-Elmer Model PE-Rx1 FTIR spectrometer with spectral resolution of 2 cm^{-1} . TEM (Hitachi Model H-7650 operated at 100 kV), SEM (Model Hitachi S-3400N) and XRD (Model: Philips X'Pert Pro Multipurpose X-ray Diffractometer) techniques were used to get detailed information about the surface morphology and structure of the prepared composites as well as of individual components.

3. Results and discussion

The prepared composites were characterized by FTIR, XRD and electron microscopic techniques. Representative TEM images of f-MWNT are displayed in figure 2a and b which

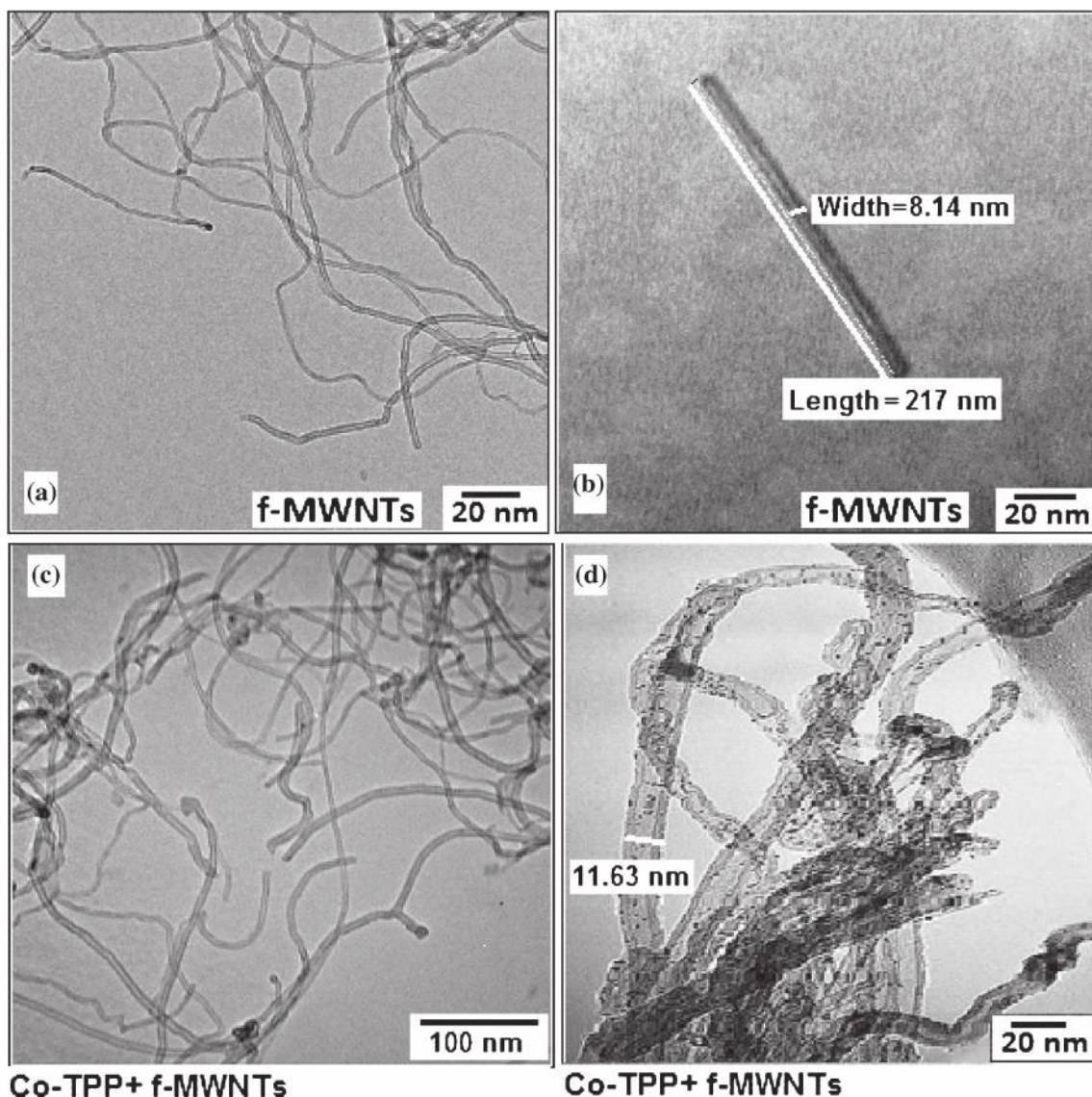


Figure 2. Transmission electron microscopic images of f-MWNT (a and b), and Co-TPP functionalized f-MWNT composite (c and d). Panels b and d provide TEM images of an isolated f-MWNT and Co-TPP functionalized f-MWNT for clarity.

indicate three-dimensional disordered arrangement of nanotubes with a mean outer diameter ranging from 8.1 to 13.0 nm and lengths up to few micrometers. Figure 2c and d indicates that nanosized clusters of aggregated Co-TPP are formed around surface of f-MWNT due to adsorption and immobilization via H-bonding, π - π and other non-covalent interactions. The TEM images of Cu-TPP and Fe-TPP functionalized MWNT nanocomposites also showed formation of nanosized clusters around the surface of MWNT.

The X-ray patterns of f-MWNT, Co-TPP and f-MWNT + Co-TPP composite as given in figure 3 do not show much shift in the low angle peak of f-MWNT at 26.45° corresponding to the (131) plane of MWNT but the relative intensity of this and few other peaks change substantially in the nanocomposite of Co-TPP functionalized MWNT, indicating

fairly strong electronic interactions between the MWNT and Co-TPP.

The major features in the IR spectra of pure Co-TPP are typical signatures of spectra of many M-TPP and the detailed vibrational analysis for the observed bands for Zn-TPP²³ and Ni-TPP²⁴ has been reported in the literature. A comparison of the IR spectra shows that bands related to the -OH stretching mode at $\sim 3436\text{ cm}^{-1}$ in the spectrum of f-MWNT become weak and shift to lower side at 3425 cm^{-1} on functionalization with Co-TPP. There are many other changes in the IR spectrum of f-MWNT + Co-TPP composite compared to the spectrum of pure Co-TPP. The IR spectrum of f-MWNT + Co-TPP in figure 1 shows shift in the position and drastic change in relative intensity of many bands compared to the bands in the spectrum of pure Co-TPP powder. The IR features observed arise mainly from pyrrole

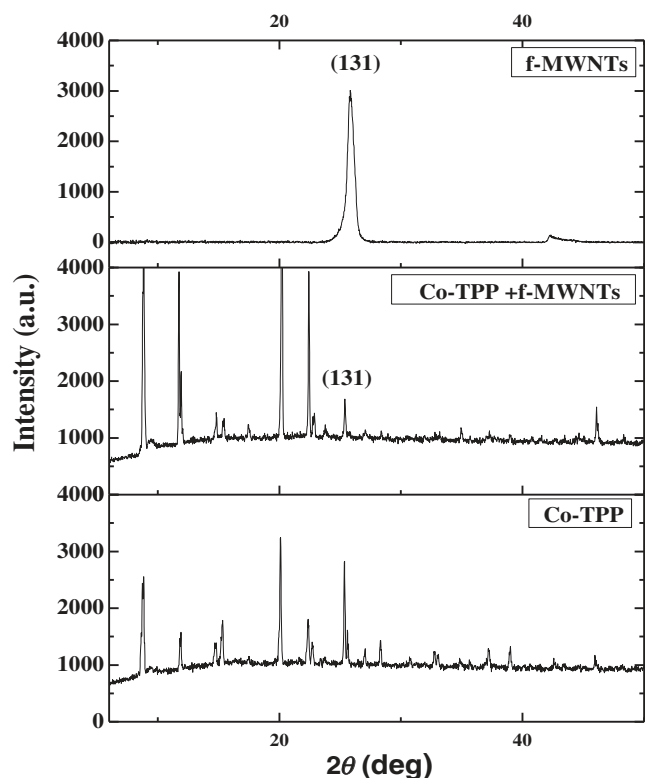


Figure 3. X-ray diffraction patterns of f-MWNT, pure Co-TPP and Co-TPP + f-MWNT nanocomposites.

units of the macrocycle. The bands at 740 and 792 cm^{-1} in the IR spectrum of Co-TPP associated with the $\gamma_{(\text{Cb}-\text{Cb}-\text{H})}$ and $\{\gamma_{(\text{Cb}-\text{Cb}-\text{H})} + \gamma_{(\text{Cb}-\text{Cb}-\text{Ca}-\text{N})}\}$ out-of-plane modes shift to 750 and 795 cm^{-1} , respectively, in the spectrum of Co-TPP + f-MWNT nanocomposite. On the other hand, there is hardly any change in the position of the IR bands at 1004 , 1071 and 1348 cm^{-1} in the spectrum of Co-TPP and Co-TPP + f-MWNT nanocomposite suggesting specific interactions between Co-TPP and f-MWNT.

The changes in the position and relative intensity of some of the bands in the IR spectra support delocalization and redistribution of π -electrons of M-TPP due to electronic interactions among f-MWNT and M-TPP. These observations along with SEM and TEM results strongly support non-covalent functionalization of MWNT with M-TPP and formation of nanosized clusters of aggregated M-TPP molecular species around the MWNT surface. The voltage vs. current response of the nanocomposite of Co-TPP functionalized f-MWNT was measured using Keithley Model 6517B electrometer. The results given in figure 4 show linear behaviour upto 5 V DC applied voltage, indicating stable character of the room temperature conductivity in this range. All our measurements on different sensors for response and recovery times were made on application of 2 V DC voltage in the linear response region.

We have conducted different experiments to determine the response and recovery times as well as to differentiate between the NB and CB vapours using the films of different

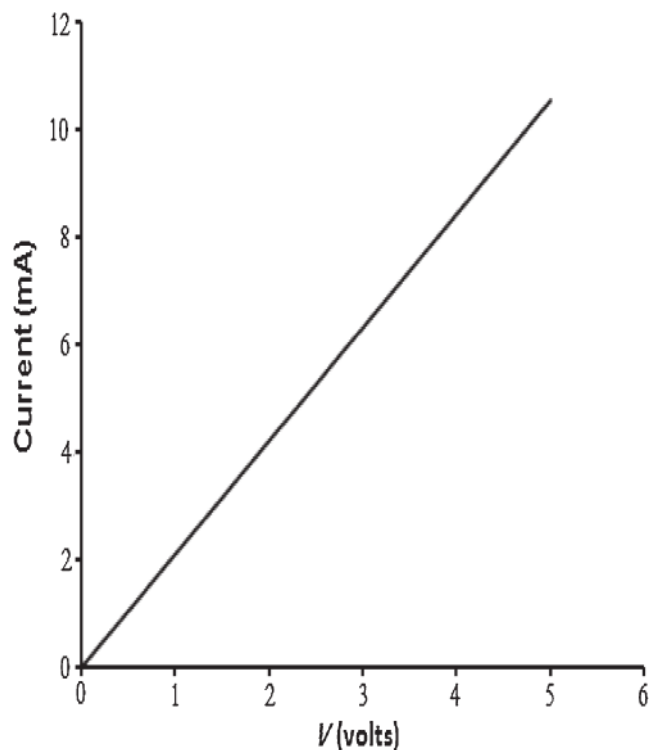


Figure 4. Current–voltage characteristics for the Co-TPP functionalized f-MWNTs nanocomposite on application of upto 5 V DC voltage.

composites. The response (S) of the sensor at a given concentration of vapour is defined as $S = \{(R - R_0)/R_0\} \times 100$, where R is the resistance of the device under exposure to target vapours and R_0 is the initial steady-state base line resistance before exposure to chemical vapours. The recovery time is defined as the time to reach 90% of total resistance change.

The metal-tetraphenylporphyrins are strongly conjugated macrocyclic systems and p -type semiconductors while the π -electron-rich MWNT may act as electron acceptor or donor depending upon the reacting species and its structure. The non-covalent interactions between f-MWNT and M-TPP result in electronic redistribution and realignment of MWNT with consequent modifications in their properties. The interactions of M-TPP functionalized f-MWNT with chemical vapours result in the partial electronic charge transfer between them affecting the position of Fermi energy and consequently the conductivity of the device.

Figure 5a and b shows the variation of resistance of the sensors based on Co-TPP functionalized f-MWNT hybrid composites on exposure to NB and CB vapours for a second under conditions described in our earlier work.²² The significant difference in the response and recovery times using Co-TPP-based devices for NB (28 and 140 s) and for CB (3 and 8 s) clearly show the potential of these devices in discriminating these two chemicals with high sensitivity. In order to check the reproducibility of our data, we conducted experiments under similar conditions and the results of repeated exposure of Co-TPP-based sensor to CB vapours at $\sim 100\text{ ppm}$

concentration are given in figure 6. This shows excellent reproducibility of our reported results. The exposure of the same sensor to different concentrations of CB vapour gives again linear response in our experiments and the details are given in figure 7. The 'on' and 'off' positions indicate the starting and closing times for exposure of chemical vapours.

In order to lend further support and to explore the possibility of likely interfering gases in discriminating capability of the device between NB and CB, we conducted studies with the films fabricated from nanohybrid materials prepared from Co-TPP functionalized f-MWNT for detection of some other chemical vapours like bromobenzene, xylene, toluene, ethanol, etc. Figure 8a and b shows the response of the sensors based on Co-TPP functionalized f-MWNT hybrid composites on exposure to bromobenzene and xylene vapours. The data for response, recovery times and change in resistance for some vapours are given in table 1. The pattern in relative change in resistance, response and recovery times on exposure to different gases is quite distinct and statistical analysis can help in discriminating between the CB and NB from one another even in the presence of some likely interfering gases.

3.1 Sensing mechanism

The functionalization of MWNT with M-TPP affects their electrical, chemical and physical properties and form nano-hybrid structures. The electronic properties of thin films

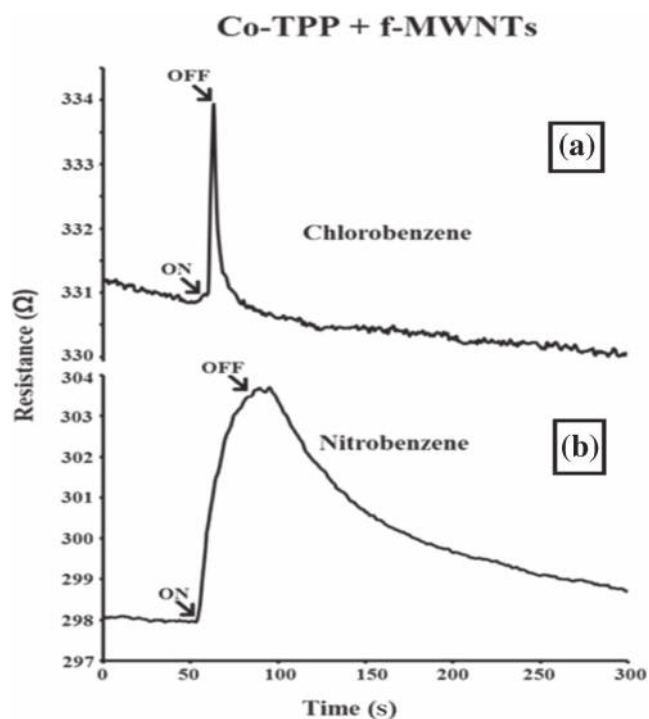


Figure 5. Response and variation of resistance of the sensors made from films of composites of Co-TPP functionalized f-MWNT on exposure to ~50 ppm concentration of chlorobenzene (a) and nitrobenzene (b) vapours respectively.

of these composites can be modulated by interaction with different gases. In our present system comprising of f-MWNT and Co-TPP, the NB and CB molecules first interact with Co-TPP which act as receptor and alters its electronic configuration. This, in turn, affects electronic configuration and alignment of conducting network of f-MWNT which is reflected in changes in electrical conductivity of the f-MWNT network.

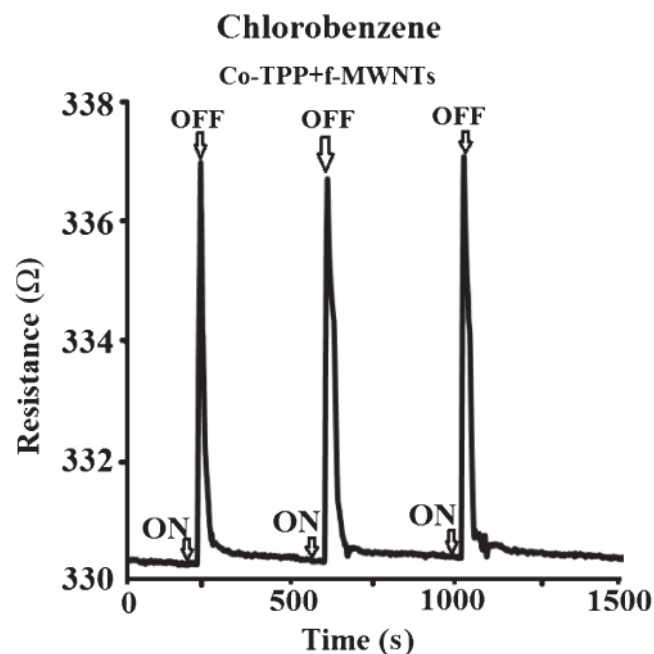


Figure 6. Response of Co-TPP functionalized f-MWNTs sensor on repeated exposure to 100 ppm concentration of chlorobenzene.

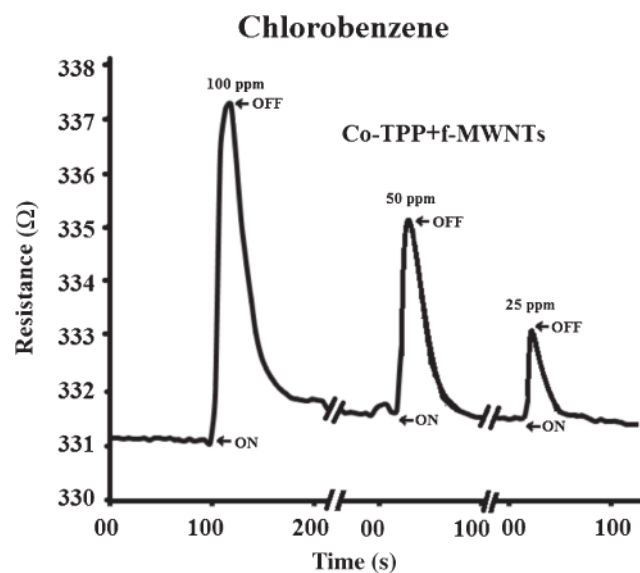
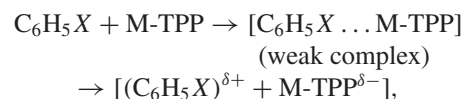


Figure 7. Response of sensor made from films of nanocomposite of Co-TPP functionalized f-MWNTs on exposure to chlorobenzene vapours at different concentrations.

The M-TPP have two possible sites for gas adsorption: one is the central metal itself and the other is the conjugated π -electronic system of the tetraphenylporphyrin macrocycle. From different chemical and physical considerations, we infer that the NB and CB molecules would interact with the periphery of the macrocycle of M-TPP. In the case of conjugated ring compounds as analytes, the main interaction route may be via the electron donating or electron accepting mechanism between the π -electrons of M-TPP and analytes. This

leads us to infer that NB and CB molecules on adsorption on the surface of M-TPP-based composite interact with the M-TPP periphery leading to partial electronic charge transfer from NB or CB molecules to M-TPP as per scheme given below



where $X = -\text{Cl}$ or $-\text{NO}_2$.

In this process, electrons are donated from NB and CB to M-TPPs producing donor states in the surface molecular layer of the film. The electron-rich M-TPP would act as donor and reduce the density of hole charge carriers in f-MWNT which behaves like a weak p -type semiconductor. The extent of charge transfer would be dependent on the type of molecule (NB or CB) and thus may lead to differential changes in the resistance, response and recovery times. Due to the presence of the NO_2 group in nitrobenzene, it may form relatively stronger bonding with M-TPP molecules and may thus lead to longer recovery time due to slow release of NB molecules from the film. The changes in electronic configuration of M-TPP on exposure and interaction with different molecules will affect the electronic configuration and conductivity of f-MWNT in the composites differently under the conditions reported here. This is what we have monitored in our experiments. The working of these devices can be satisfactorily explained in this frame work.

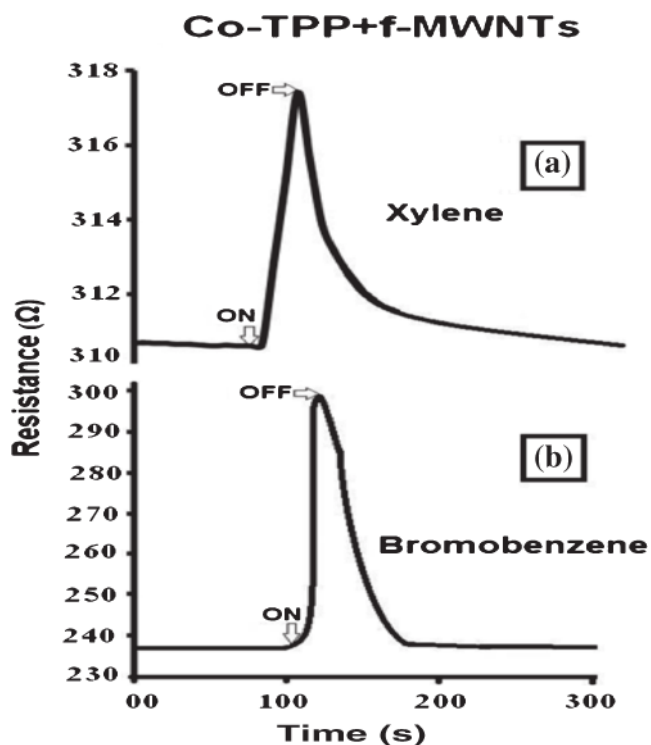


Figure 8. Response and variation of resistance of the sensors made from films of hybrid composites of Co-TPP functionalized f-MWNT on exposure to ~ 50 ppm concentration of xylene (a) and bromobenzene (b) vapours.

4. Conclusions

A process for preparation of nanocomposites by non-covalent functionalization of CNTs with metal-tetraphenylporphyrins (M-TPP) is discussed. Formation of nano-sized clusters of aggregated M-TPP around the f-MWNT surface is clearly indicated by the TEM and FTIR techniques. The prepared devices show differential changes in resistance, response and

Table 1. Change in resistance, response and recovery times for Cu-TPP and Co-TPP functionalized MWNT nano-composite-based sensors on exposure to ~ 50 ppm concentration of different chemical vapours.

Type of vapours	% Change in resistance (Ω) ($\Delta R/R_0$) $\times 100$		Response time (s)		Recovery time (s)	
	CuTPP + f-MWNT	CoTPP + f-MWNT	CuTPP + f-MWNT	CoTPP + f-MWNT	CuTPP + f-MWNT	CoTPP + f-MWNT
	Benzene	4	1.7	6	4	$\sim 42^a$
Toluene	6.8	1.1	5	10	$\sim 46^a$	13
Xylene	6.3	3.1	6	10	$\sim 48^a$	35
Nitrobenzene	8	3	8	28	124	140
Chlorobenzene	17	1	6	3	$\sim 42^a$	8
Bromobenzene	18	23	19	14	$\sim 44^a$	45
Chloroform	1.7	2.9	86	125	305	62
Ethanol	6	2.2	20	21	21	24

^aThe de-adsorption of vapours from the Cu-TPP functionalized MWNT device after exposure to BTX vapours is very slow after ~ 30 s and therefore the recovery times given in the table are the best estimated values.

recovery times on exposure to NB, CB and some other chemical vapours. A comparison of the data in table 1 clearly shows a distinct response pattern for CB and NB vapours making their identification feasible. The MWNTs form transducing part of the device fabricated from the M-TPP functionalized MWNT-based nanocomposites. The interesting features of these devices are that they can be coated on the glass, plastics or irregular shaped materials, easy to fabricate, have fast response and recovery times, operate at room temperature and are highly reproducible with long-term stability of more than 6 months for identification of chemical vapours.

Acknowledgement

Financial support for this work by Amity Science, Technology and Innovation Foundation, New Delhi is gratefully acknowledged.

References

1. Cao H B, Li Y P, Zhang G F and Zhang Y 2004 *Biotechnol. Lett.* **26** 307
2. Zhao L, Ma J and Sun Z Z 2008 *Appl. Catal. B* **79** 244
3. Ye J, Singh A and Ward O P 2004 *J. Microbiol. Biotechnol.* **20** 117
4. Mu Y, Yu H Q, Zheng J C, Zhang S J and Sheng G P 2004 *Chemosphere* **54** 789
5. Oh Y S and Bartha R 1994 *Appl. Environ. Microbiol.* **60** 2717
6. Fu T 2011 *Anal. Bioanal. Chem.* **401** 1167
7. Algarra M, Campos B B, Miranda M S and Esteves da Silva J C G 2011 *Talanta* **83** 1335
8. Cui S, Liu X Y, Liu Y, Shen X D, Lin B L, Han G F and Wu Z W 2010 *Sci. China Technol. Sci.* **53** 2367
9. Ali T 2006 *J. Chromatogr. A* **1125** 129
10. Wang Y and Lee H K 1998 *J. Chromatogr. A* **803** 219
11. Reyhaneh R K, Yaghoub A, Farzaneh S, Mohammad-Reza M H and Mohammad R J 2007 *Talanta* **72** 387
12. Langhorst M L and Nestruck T J 1979 *Anal. Chem.* **51** 2018
13. Wang L, Teleki A, Pratsinis S E and Gouma P I 2008 *Chem. Mater.* **20** 4794
14. Yang L, Saavedra S S and Armstrong N R 1996 *Anal. Chem.* **68** 1834
15. Leghrib R and Llobet E 2011 *Anal. Chim. Acta* **708** 19
16. Penza M, Rossi R, Alvisi M, Cassano G and Serra E 2009 *Sens. Actuators B: Chem.* **140** 176
17. Penza M, Rossi R, Alvisi M, Valerini D, Serra E, Paolesse R, Martinelli E, Amico A D' and Natale C D 2009 *Procedia Chem.* **1** 975
18. Verma A L, Saxena S, Saini G S S, Gaur V and Jain V K 2011 *Thin Solid Films* **519** 8144
19. Penza M, Rossi R, Alvisi M, Signore M A, Serra E, Paolesse R, Amico A D' and Natale C Di 2010 *Sens. Actuators B* **144** 387
20. Shi D W, Wei L M, Wang J, Zhao J, Chen C X, Xu D, Geng H J and Zhang Y F 2013 *Sens. Actuators B* **177** 370
21. Rushi, A, Datta K, Ghosh P, Mulchandani A and Shirsat M D 2013 *Mater. Lett.* **96** 38
22. Saxena S and Verma A L 2014 *Adv. Mater. Lett.* **5** 472
23. Saini G S S, Dogra S D, Singh G, Tripathi S K, Kaur S, Sathe V and Choudhary B C 2012 *Vib. Spectrosc.* **61** 188
24. Rush T S III, Kozlowski P M, Piffat C A, Kumble R, Zgierski M Z and Spiro T G 2000 *J. Phys. Chem. B* **104** 5020